



PAPER • OPEN ACCESS

Non-adiabatic holonomic quantum computation

To cite this article: Erik Sjöqvist *et al* 2012 *New J. Phys.* **14** 103035

View the [article online](#) for updates and enhancements.

Related content

- [Universal non-adiabatic geometric manipulation of pseudo-spin charge qubits](#)
Vahid Azimi Mousolou
- [Universal non-adiabatic holonomic gates in quantum dots and single-molecule magnets](#)
Vahid Azimi Mousolou, Carlo M Canali and Erik Sjöqvist
- [Shortcuts to adiabatic holonomic quantum computation in decoherence-free subspace with transitionless quantum driving algorithm](#)
Xue-Ke Song, Hao Zhang, Qing Ai et al.

Recent citations

- [Multiple-qubit controlled unitary quantum gate for Rydberg atoms using shortcut to adiabaticity and optimized geometric quantum operations](#)
Meng Li *et al*
- [Implementation of Geometric Quantum Gates on MicrowaveDriven Semiconductor Charge Qubits](#)
Chengxian Zhang *et al*
- [Distinguishment of Greenberger–Horne–Zeilinger States in Rydberg Atoms via Noncyclic Geometric Quantum Computation](#)
FuQiang Guo *et al*

Non-adiabatic holonomic quantum computation

Erik Sjöqvist^{1,2}, D M Tong³, L Mauritz Andersson⁴,
Björn Hessmo¹, Markus Johansson^{1,2} and Kuldip Singh¹

¹ Centre for Quantum Technologies, National University of Singapore,
3 Science Drive 2, 117543 Singapore, Singapore

² Department of Quantum Chemistry, Uppsala University, Box 518,
SE-751 20 Uppsala, Sweden

³ Physics Department, Shandong University, Jinan 250100, China

⁴ Department of Applied Physics, KTH Royal Institute of Technology,
SE-100 44 Stockholm, Sweden

E-mail: erik.sjoqvist@kvac.uu.se, tdm@sdu.edu.cn, mauritza@kth.se,
phyhbg@nus.edu.sg, cqtbemj@nus.edu.sg and sciks@nus.edu.sg

New Journal of Physics **14** (2012) 103035 (10pp)

Received 20 August 2012

Published 23 October 2012

Online at <http://www.njp.org/>

doi:10.1088/1367-2630/14/10/103035

Abstract. We develop a non-adiabatic generalization of holonomic quantum computation in which high-speed universal quantum gates can be realized using non-Abelian geometric phases. We show how a set of non-adiabatic holonomic one- and two-qubit gates can be implemented by utilizing optical transitions in a generic three-level Λ configuration. Our scheme opens up the possibility of realizing universal holonomic quantum computation on qubits characterized by short coherence time.



Content from this work may be used under the terms of the [Creative Commons Attribution-NonCommercial-ShareAlike 3.0 licence](https://creativecommons.org/licenses/by-nc-sa/3.0/). Any further distribution of this work must maintain attribution to the author(s) and the title of the work, journal citation and DOI.

Contents

1. Introduction	2
2. Non-adiabatic holonomic quantum computation	3
3. Physical implementation	4
3.1. One-qubit gate	4
3.2. Two-qubit gate	5
3.3. Robustness to decay	6
4. Geometric interpretation	8
5. Conclusions	9
Acknowledgments	9
References	10

1. Introduction

Circuit-based quantum computation relies on the ability to perform a universal set of quantum gate operations on a set of quantum-mechanical bits (qubits). A key challenge in achieving this goal is to find implementations of gates that are resilient to certain kinds of errors. Holonomic quantum computation (HQC) [1] is a general procedure for building universal sets of robust gates using non-Abelian geometric phases [2].

HQC is conventionally based on adiabatic evolution. The idea is to encode a set of qubits in a set of degenerate eigenstates of a parameter-dependent Hamiltonian and to adiabatically transport these states around a loop in the corresponding parameter space. This effectuates a holonomic gate acting on the qubits. It has been shown [1] that adiabatic quantum holonomies generically allow for universal quantum computation.

Adiabatic holonomic gates have been proposed for trapped ions [3], superconducting nanocircuits [4] and semiconductor quantum dots [5]. These gates still await experimental realization. An obstacle in achieving this is the long run time required for the desired parametric control associated with adiabatic evolution. In other words, as these gates operate slowly compared to the dynamical time scale, they become vulnerable to open system effects and parameter fluctuations that may lead to loss of coherence. On the other hand, if the run time is decreased in order to shorten the exposure, non-adiabatic corrections start to become significant and parametric control is lost. These problems have been tackled [6] by using Abelian non-adiabatic geometric phases [7] to realize quantum gates. However, such geometric phase gates are limited to commuting operations and thus cannot perform universal HQC.

To combine speed and universality, we propose here a generalization of HQC based on the non-adiabatic non-Abelian geometric phases proposed in [8]. The key advantage of our holonomic setting is that it removes the problem of long run time associated with the original form of HQC [1]. We demonstrate an experimentally feasible optical scheme to implement a universal set of holonomic one- and two-qubit gates for non-adiabatic optical transitions in three-level Λ configurations. The proposed setup allows for any quantum computation on any number of qubits by purely geometric means.

The outline of the paper is as follows. The general theory of non-adiabatic HQC is described in the next section. In section 3, we demonstrate a universal set of non-adiabatic holonomic gates in a generic Λ configuration and show that these gates can be made robust to

decay. The non-adiabatic holonomic gates are interpreted geometrically in section 4. The paper ends with the conclusions.

2. Non-adiabatic holonomic quantum computation

Consider a quantum system characterized by an N -dimensional Hilbert space. A computational system, typically a set of qubits, is encoded in a K -dimensional subspace $M(0)$ of Hilbert space. A quantum gate that manipulates the computational state can be induced by taking $M(0)$ around a smooth path $C : [0, \tau] \ni t \mapsto M(t)$ of K -dimensional subspaces in such a way that $M(\tau) = M(0)$. Thus, C is a loop of such subspaces generated by a suitable Hamiltonian $H(t)$ of the full system. In this way, any computational state residing in $M(0)$ will, in general, end up in a new state in the same subspace. The unitary transformation relating the final and initial states is the quantum gate. The idea of non-adiabatic HQC is to make the resulting gate C dependent, but independent of any dynamical parameters such as the run time τ and the energies of the system.

Let us formalize this idea by introducing a once differentiable set of orthonormal ordered bases $|\zeta_k(t)\rangle$, $k = 1, \dots, K$, of $M(t)$ along C , such that $|\zeta_k(\tau)\rangle = |\zeta_k(0)\rangle$. One may visualize $|\zeta_k(t)\rangle$ as a K -tuple of vectors moving in the N -dimensional Hilbert space of the full system. The final time evolution operator projected onto the initial subspace may be written as ($\hbar = 1$ from now on) [8]

$$U(\tau, 0) = \sum_{k,l=1}^K \left(\mathbf{T} e^{i \int_0^\tau (A(t) - \mathbf{H}(t)) dt} \right)_{kl} |\zeta_k(0)\rangle \langle \zeta_l(0)|, \quad (1)$$

where \mathbf{T} is time ordering. Here, $A_{kl}(t) = i \langle \zeta_k(t) | \dot{\zeta}_l(t) \rangle$ and $\mathbf{H}_{kl}(t) = \langle \zeta_k(t) | H(t) | \zeta_l(t) \rangle$ are Hermitian $K \times K$ matrices. Thus, $U(\tau, 0)$ is a unitary operator on $M(0)$.

To understand the meaning of A , let us check how it transforms under a smooth change of basis spanning $M(t)$. Such a transformation is known as a gauge transformation as it changes the basis but not the subspace itself. Explicitly, if $|\zeta_k(t)\rangle \rightarrow \sum_{l=1}^K |\zeta_l(t)\rangle V_{lk}(t)$, $V(t)$ being a once differentiable family of unitary $K \times K$ matrices such that $V(\tau) = V(0)$, then $A \rightarrow V^\dagger A V + i V^\dagger \dot{V}$. This shows that A transforms as a proper vector potential. Thus, the unitary

$$U = \mathbf{P} e^{i \oint_C \mathcal{A}}, \quad (2)$$

$\mathcal{A}_{kl} = i \langle \zeta_k(t) | d\zeta_l(t) \rangle$ being the matrix-valued connection one-form, is the holonomy matrix generalizing the Wilczek–Zee holonomy [2] to non-adiabatic evolutions. Note that \mathbf{P} is path ordering along C and that $U \rightarrow V^\dagger(0) U V(0)$ under a gauge transformation. This gauge covariance essentially means that the holonomy matrix is a property of the loop C and we may write $U \equiv U(C)$.

The following two conditions are necessary for universal non-adiabatic HQC: (i) there should exist physically accessible loops C of subspaces along which the Hamiltonian matrix $\mathbf{H}_{kl}(t) = \langle \zeta_k(t) | H(t) | \zeta_l(t) \rangle$ vanishes; and (ii) there should exist at least two such loops C and C' , both based at $M(0)$, for which the corresponding $U(C)$ and $U(C')$ do not commute. While the first condition ensures that the evolution is purely geometric, the second one is necessary to realize universality. Under conditions (i) and (ii), there is a set of quantum gates

$$U(\tau, 0) = U(C) = \sum_{k,l=1}^K U_{kl}(C) |\zeta_k(0)\rangle \langle \zeta_l(0)| \quad (3)$$

that may be able to perform any computation on qubits encoded in $M(0)$ based purely on the geometric properties of the subspace paths. We demonstrate that these conditions can be met in a generic three-level Λ configuration by means of which a universal set of one- and two-qubit gates can be realized.

3. Physical implementation

3.1. One-qubit gate

Consider a three-level atom or ion consisting of the ‘bare’ energy eigenstates $|0\rangle$, $|1\rangle$ and $|e\rangle$ with energies w_0 , w_1 and w_e , respectively. These states form a Λ configuration in which each $k \leftrightarrow e$ transition ($k = 0, 1$) is driven separately by a suitably polarized laser pulse with frequency ν_k . In the rotating frame, the Hamiltonian describing the system–laser interaction takes the form

$$H(t) = \Delta_0|0\rangle\langle 0| + \Delta_1|1\rangle\langle 1| + \Omega(t) (\omega_0|e\rangle\langle 0| + \omega_1|e\rangle\langle 1| + \text{h.c.}), \quad (4)$$

where we have neglected rapidly oscillating counter-rotating terms (rotating wave approximation). Here, $\Delta_k = 2\pi\nu_k - \omega_{ek}$, where $\omega_{ek} = w_e - w_k$, are detunings that can be varied independently by changing ν_k . The laser parameters ω_0 and ω_1 satisfy $|\omega_0|^2 + |\omega_1|^2 = 1$, and describe the relative strength and relative phase of the $0 \leftrightarrow e$ and $1 \leftrightarrow e$ transitions. The Hamiltonian is turned on and off at $t = 0$ and $t = \tau$, respectively, controlled by the pulse envelope $\Omega(t)$. We take $|0\rangle$ and $|1\rangle$ to define the one-qubit state space $M(0)$.

A universal holonomic one-qubit gate can be realized in the above Λ system by choosing time-independent ω_0 and ω_1 over the duration of the pulse pair and by tuning the laser frequencies so that the detunings Δ_0 and Δ_1 vanish. Under these conditions, the Hamiltonian reduces to

$$H^{(1)}(t) = \Omega(t) (\omega_0|e\rangle\langle 0| + \omega_1|e\rangle\langle 1| + \text{h.c.}) \quad (5)$$

with the corresponding coupling structure shown in figure 1. Given this choice of laser pulses, the dark state $|d\rangle = -\omega_1|0\rangle + \omega_0|1\rangle$ decouples from the dynamics, which in turn implies that the evolution is reduced to a simple Rabi oscillation between the bright state $|b\rangle = \omega_0^*|0\rangle + \omega_1^*|1\rangle$ and the excited state [9]. The Rabi frequency is $\Omega(t)$. It follows that the qubit subspace $M(0)$ evolves into $M(t)$ spanned by $|\psi_k(t)\rangle = e^{-i\int_0^t H^{(1)}(t')dt'}|k\rangle = U(t, 0)|k\rangle$, $k = 0, 1$, which undergoes cyclic evolution if the pulse pair satisfies $\int_0^\tau \Omega(t')dt' = \pi$. The evolution is purely geometric since $\langle\psi_k(t)|H^{(1)}(t)|\psi_l(t)\rangle = \langle k|H^{(1)}(t)|l\rangle = 0$ for $t \in [0, \tau]$. Under the above conditions, the final time evolution operator $U(\tau, 0)$ projected onto the computational space spanned by $\{|0\rangle, |1\rangle\}$ defines the holonomic one-qubit gate

$$U^{(1)}(C_{\mathbf{n}}) = \mathbf{n} \cdot \boldsymbol{\sigma}, \quad (6)$$

where \mathbf{n} is a unit vector in \mathbb{R}^3 and $\boldsymbol{\sigma} = (\sigma_x, \sigma_y, \sigma_z)$ are the standard Pauli operators acting on $|0\rangle$ and $|1\rangle$. By letting $\omega_0 = \sin(\theta/2)e^{i\phi}$ and $\omega_1 = -\cos(\theta/2)$, we find that $\mathbf{n} = (\sin\theta \cos\phi, \sin\theta \sin\phi, \cos\theta)$. $U^{(1)}(C_{\mathbf{n}})$ is a universal one-qubit gate. This can be seen explicitly by noting that two pairs of laser pulses corresponding to the unit vectors \mathbf{n} and \mathbf{m} applied sequentially result in

$$U^{(1)}(C) = U^{(1)}(C_{\mathbf{m}})U^{(1)}(C_{\mathbf{n}}) = \mathbf{n} \cdot \mathbf{m} - i\boldsymbol{\sigma} \cdot (\mathbf{n} \times \mathbf{m}). \quad (7)$$

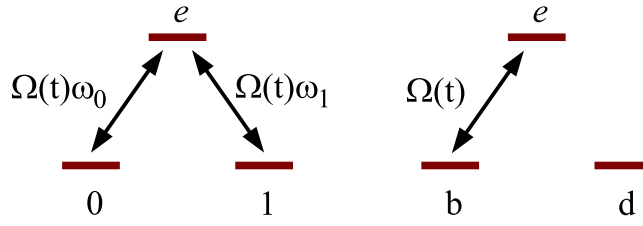


Figure 1. Setup for non-adiabatic holonomic one-qubit gate in a Λ configuration. A pair of zero-detuned laser pulses couple two ground state levels 0 and 1 to an excited state e (left panel). The two ground state levels define a single qubit and the laser parameters satisfy $|\omega_0|^2 + |\omega_1|^2 = 1$. Note that the ‘bare’ ground state levels may be degenerate or non-degenerate since the lasers are assumed to be tunable in an independent fashion. The dark state $|d\rangle = -\omega_1|0\rangle + \omega_0|1\rangle$ is decoupled from the bright state $|b\rangle = \omega_0^*|0\rangle + \omega_1^*|1\rangle$ by choosing time-independent ω_0 and ω_1 over the duration of the pulse pair. The system thereby performs Rabi oscillations between the bright and excited states with frequency $\Omega(t)$ (right panel). The evolution of the qubit subspace is purely geometric and becomes cyclic after completing a Rabi oscillation by choosing $\Omega(t)$ to be a real-valued π pulse. The resulting unitary quantum gate operation acting on the qubit is determined by the holonomy of the loop traced out by the subspace spanned by $e^{-i\int_0^t H^{(1)}(t')dt'}|k\rangle$, $k = 0, 1$. By applying sequentially two π pulse pairs with negligible temporal overlap, any desired holonomic one-qubit gate can be realized.

This is an $SU(2)$ transformation corresponding to a rotation of the qubit by an angle $2 \arccos(\mathbf{n} \cdot \mathbf{m})$ around the normal of the plane spanned by \mathbf{n} and \mathbf{m} . Here, $C_{\mathbf{n}}$ and $C_{\mathbf{m}}$ are loops based at $M(0)$ and $C = C_{\mathbf{m}} \circ C_{\mathbf{n}}$. By suitable choices of \mathbf{n} and \mathbf{m} , any desired one-qubit gate can be realized. For instance, the choice $\mathbf{n} = (\cos \phi, \sin \phi, 0)$ and $\mathbf{m} = (\cos \phi', \sin \phi', 0)$ results in the phase shift gate $|k\rangle \mapsto e^{2ik(\phi' - \phi)}|k\rangle$, $k = 0, 1$, up to an unimportant overall phase factor. A Hadamard gate $|k\rangle \mapsto \frac{1}{\sqrt{2}}[(-1)^k|k\rangle + |k \oplus 1\rangle]$, $k = 0, 1$, can be implemented by a single pulse with $\mathbf{n} = \frac{1}{\sqrt{2}}(1, 0, 1)$.

3.2. Two-qubit gate

To complete the universal set, we propose a physical realization of a non-adiabatic holonomic two-qubit gate in an ion trap setup. Our scheme is a non-adiabatic version of [3], which utilizes the Sørensen–Mølmer setting [10] to design a holonomic two-qubit gate. The system consists of an array of trapped ions, each of which exhibits an internal three-level structure 0, 1 and e . The transitions $0 \leftrightarrow e$ and $1 \leftrightarrow e$ for an ion pair in the array are addressed by lasers with detunings $\pm\nu \pm \delta$ and $\pm\nu \mp \delta$, respectively, where ν is a phonon frequency and δ is an additional detuning. Off-resonant couplings to the singly excited states $|e0\rangle$, $|0e\rangle$, $|e1\rangle$ and $|1e\rangle$ can be suppressed by choosing the Rabi frequencies $|\Omega_0(t)|$ and $|\Omega_1(t)|$ smaller than ν [10]. In this way, the effective two-ion Hamiltonian in the Lamb–Dicke regime reads

$$H^{(2)} = \frac{\eta^2}{\delta} (|\Omega_0(t)|^2 \sigma_0(\phi) \otimes \sigma_0(\phi) - |\Omega_1(t)|^2 \sigma_1(-\phi) \otimes \sigma_1(-\phi)). \quad (8)$$

Here, η is the Lamb–Dicke parameter ($\eta^2 \ll 1$), $\sigma_0(\phi) = e^{i\phi/4}|e\rangle\langle 0| + \text{h.c.}$ and $\sigma_1(-\phi) = e^{-i\phi/4}|e\rangle\langle 1| + \text{h.c.}$ Note that due to the non-adiabatic nature of our gate, the ancilla state a of the original adiabatic scheme in [3] is no longer needed. The phase ϕ and the ratio $|\Omega_0(t)|^2/|\Omega_1(t)|^2 = \tan(\theta/2)$ should be kept constant during each pulse pair. By expanding $\sigma_0(\phi)$ and $\sigma_1(-\phi)$, the Hamiltonian $H^{(2)}$ can be decomposed as

$$H^{(2)} = \frac{\eta^2}{\delta} \sqrt{|\Omega_0(t)|^4 + |\Omega_1(t)|^4} (H_0 + H_1). \quad (9)$$

The two terms

$$\begin{aligned} H_0 &= \sin \frac{\theta}{2} e^{i\phi/2} |ee\rangle \langle 00| - \cos \frac{\theta}{2} e^{-i\phi/2} |ee\rangle \langle 11| + \text{h.c.}, \\ H_1 &= \sin \frac{\theta}{2} |e0\rangle \langle 0e| - \cos \frac{\theta}{2} |e1\rangle \langle 1e| + \text{h.c.} \end{aligned} \quad (10)$$

commute, which implies that

$$e^{-i \int_0^\tau H^{(2)}(t) dt} = e^{-i\pi H_0} e^{-i\pi H_1} \quad (11)$$

under the π pulse criterion $\frac{\eta^2}{\delta} \int_0^\tau \sqrt{|\Omega_0(t)|^4 + |\Omega_1(t)|^4} dt = \pi$. The second factor $e^{-i\pi H_1}$ on the right-hand side of the time-evolution operator in (11) acts trivially on the computational subspace spanned by $\{|00\rangle, |01\rangle, |10\rangle, |11\rangle\}$. Thus, $H^{(2)}$ effectively reduces to the Λ -like Hamiltonian $\frac{\eta^2}{\delta} \sqrt{|\Omega_0(t)|^4 + |\Omega_1(t)|^4} H_0$ from which the holonomic two-qubit gate

$$\begin{aligned} U^{(2)}(C_n) &= \cos \theta |00\rangle \langle 00| + \sin \theta e^{-i\phi} |00\rangle \langle 11| + \sin \theta e^{i\phi} |11\rangle \langle 00| - \cos \theta |11\rangle \langle 11| \\ &\quad + |01\rangle \langle 01| + |10\rangle \langle 10| \end{aligned} \quad (12)$$

follows by analogy of the single-qubit gate above. The path C_n , being characterized by the unit vector $\mathbf{n} = (\sin \theta \cos \phi, \sin \theta \sin \phi, \cos \theta)$ in \mathbb{R}^3 , is traversed in the three-dimensional subspace spanned by $\{|00\rangle, |11\rangle, |ee\rangle\}$ of the internal degrees of freedom of the ions. For instance, a conditional phase shift gate $|kl\rangle \mapsto e^{ikl\pi} |kl\rangle$, $k, l = 0, 1$, can be implemented by choosing $\theta = 0$. Due to its entangling nature, $U^{(2)}(C_n)$ is universal when assisted by one-qubit gates [11].

3.3. Robustness to decay

In practical implementations utilizing atomic or ionic systems, $|0\rangle$ and $|1\rangle$ typically correspond to stable ground states, while the excited state $|e\rangle$ is unstable. Since the excited state is significantly populated in the non-adiabatic scheme, it is important to check its robustness to the error caused by the finite lifetime of e . To test this, we add decay of e to the non-adiabatic holonomic gates. We compare the resulting fidelity with that of the corresponding adiabatic gate. As a test case, we choose the one-qubit phase shift gate $|k\rangle \rightarrow e^{ik\pi/2} |k\rangle$, $k = 0, 1$, in the non-adiabatic and adiabatic scenarios. This gate can be implemented adiabatically utilizing the Λ -type system, but now by varying the two laser couplings independently so as to remain approximately in an instantaneous dark state in the limit of large run time T . We assume that the excited state decays to the auxiliary ground state level $|g\rangle$ with rate γ . We model the decay with the Lindblad equation

$$\dot{\varrho}_t = -i[H^{(1)}(t), \varrho_t] + 2L\varrho_t L^\dagger - L^\dagger L\varrho_t - \varrho_t L^\dagger L, \quad (13)$$

where ϱ_t is the density operator and $L = \sqrt{\gamma}|g\rangle\langle e|$. Furthermore, $H^{(1)}(t) = \Omega(t)(\omega_0|e\rangle\langle 0| + \omega_1|e\rangle\langle 1| + \text{h.c.})$ and $H^{(1)}(t) = \Omega(\omega_1(t/T)|e\rangle\langle 1| + \omega_a(t/T)|e\rangle\langle a| + \text{h.c.})$ are the Hamiltonians in

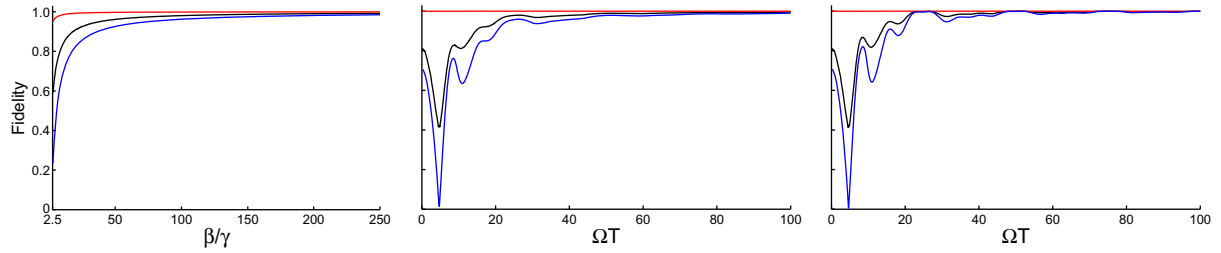


Figure 2. Influence of decay with rate γ of the excited state e on the non-adiabatic and adiabatic holonomic phase shift gate $|k\rangle \rightarrow e^{ik\pi/2}|k\rangle$, $k = 0, 1$. The effect is quantified in terms of minimum (blue), average (black) and maximum (red) fidelities. The three panels show, from left to right, the non-adiabatic gate with decay, the adiabatic gate with decay and the adiabatic gate without decay. Choosing hyperbolic secant π pulses with amplitude β , the non-adiabatic fidelities are shown as functions of the dimensionless quantity β/γ . We show the adiabatic fidelities as functions of the dimensionless quantity ΩT , where Ω is the time-independent global strength of laser couplings and T is the run time of the gate. We have chosen $\Omega/\gamma = 12.5$ and $\gamma \Delta t = 8$, where Δt is the temporal separation of the two laser pulses in the non-adiabatic setting. Δt is chosen to be sufficiently large to guarantee negligible pulse overlap for the β/γ range shown in the left panel.

the non-adiabatic and adiabatic settings, respectively. In the adiabatic case, note that the 0-state is decoupled from the excited state and that the a state is another ancillary ground state level [3]. Two hyperbolic secant π pulse pairs are chosen to implement the non-adiabatic phase shift gate. Explicitly, we choose $\Omega(t) (\omega_0, \omega_1) = \beta \operatorname{sech}(\beta t)(-1, 1)/\sqrt{2}$ and $\Omega(t - \Delta t) (\omega'_0, \omega'_1) = \beta \operatorname{sech}[\beta(t - \Delta t)](-1, e^{-i\pi/4})/\sqrt{2}$, where β is the amplitude of the pulses and Δt is the temporal separation of the two pulse pairs. The ideal adiabatic gate is generated in the $T \rightarrow \infty$ limit by varying the laser couplings $\omega_1 = \sin(\vartheta/2)e^{i\varphi}$ and $\omega_a = -\cos(\vartheta/2)$ along the loop $(\vartheta, \varphi) = (0, 0) \rightarrow (\pi/2, 0) \rightarrow (\pi/2, \pi) \rightarrow (0, \pi) \rightarrow (0, 0)$ at constant speed.

In figure 2, we show the fidelity $\langle \xi | U^\dagger(C) \varrho_{\text{out}} U(C) | \xi \rangle$, computed numerically for 4000 input states $|\xi\rangle$, uniformly distributed over the Bloch sphere. Here, $U(C)$ is the non-adiabatic or adiabatic holonomic gate and ϱ_{out} is the output state computed from equation (13). The fidelities are shown as functions of the dimensionless quantities β/γ and ΩT in the non-adiabatic and adiabatic cases, respectively. Note that the pulse duration in the non-adiabatic setting decreases with increasing β/γ since the pulse area is set to the fixed value π . Thus, by increasing β/γ we effectively speed up the gate. Furthermore, we have chosen $\Omega/\gamma = 12.5$ and $\gamma \Delta t = 8$, where the latter choice guarantees that the pulse overlap is negligible for the β/γ range shown in the figure, a necessary condition to avoid any spurious dynamical contributions to the gate.

The fidelities of the non-adiabatic gate tend monotonically to unity in the large β/γ limit (left panel). This demonstrates that the non-adiabatic version of the holonomic phase shift gate can be made robust to decay of the excited state by employing sufficiently short pulses. A key point with adiabatic HQC is that the population of the decaying excited state becomes negligible in the adiabatic limit. This behavior is confirmed as the fidelities of the adiabatic gate in the presence of decay tend to unity in the large- T limit (middle panel). The oscillatory behavior, on

the other hand, is due to non-adiabatic effects originating from the finite run time of the gate and is thus present also when the decay is set to zero (right panel). The revivals seen in the fidelities of the adiabatic gate without decay have been pointed out previously [12, 13].

Other types of errors may affect the gate fidelities. In a separate publication [14], we consider the effect of dephasing (of relevance to superconducting qubits) and different types of parameter errors on non-adiabatic and adiabatic holonomic gates.

4. Geometric interpretation

To understand the nature of the above holonomic gates, we need to introduce a few concepts from differential geometry. A Grassmann manifold $G(N; K)$ is the set of K -dimensional subspaces of an N -dimensional Hilbert space. It is isomorphic to the set of complex K -planes in \mathbb{C}^N . The closed path C of K -dimensional subspaces is a loop in $G(N; K)$. The set of all bases forms a Stiefel manifold $\mathcal{S}(N; K)$, which is a fiber bundle with $G(N; K)$ as base manifold and with the set of $K \times K$ unitary matrices as fibers [15]. A lift of the loop C in $G(N; K)$ to a loop \mathcal{C} in $\mathcal{S}(N; K)$ corresponds to a single-valued choice of gauge. A gauge transformation is a unitary change of bases over C . The unitary $U(C)$ in equation (2) is the holonomy matrix associated with the loop C in $G(N; K)$.

Now, let us consider the holonomic one- and two-qubit gates described in section 3. These gates are associated with loops in $G(3; 2)$, where the Hilbert spaces relevant for the holonomies are spanned by $\{|0\rangle, |1\rangle, |e\rangle\}$ and $\{|00\rangle, |11\rangle, |ee\rangle\}$ in the one- and two-qubit cases, respectively. We lift the loop C_n in $G(3; 2)$ to a loop \mathcal{C}_n in $\mathcal{S}(3; 2)$. As noted above, each such lift corresponds to a choice of gauge. In the one-qubit case, the loop C_n may be represented by a set of complex two-planes spanned by the single-valued vectors

$$\begin{aligned} |\zeta_1(t)\rangle &= U(t, 0)|d\rangle = |d\rangle, \\ |\zeta_2(t)\rangle &= e^{i\delta(t)}U(t, 0)|b\rangle = e^{i\delta(t)}[\cos\delta(t)|b\rangle - i\sin\delta(t)|e\rangle] \end{aligned} \quad (14)$$

in the three-dimensional complex vector space \mathbb{C}^3 . Here, $\delta(t) = \int_0^t \Omega(t') dt'$ and the global phase factor $e^{i\delta(t)}$ has been inserted to ensure that $|\zeta_2(\tau)\rangle = |\zeta_2(0)\rangle$. The same expressions for $|\zeta_1(t)\rangle$ and $|\zeta_2(t)\rangle$ apply to the two-qubit case by making the replacements $|d\rangle \rightarrow \cos(\theta/2)|00\rangle + \sin(\theta/2)e^{i\phi}|11\rangle$, $|b\rangle \rightarrow \sin(\theta/2)e^{-i\phi}|00\rangle - \cos(\theta/2)|11\rangle$ and $|e\rangle \rightarrow |ee\rangle$. The loop C_n can be visualized by noting that $|\zeta_1\rangle$ points in a fixed direction in \mathbb{C}^3 around which $|\zeta_2\rangle$ rotates. Physically, $|\zeta_1\rangle$ represents the dark state and $|\zeta_2\rangle$ describes the Rabi oscillations between the bright and excited states [9]. The oscillations correspond to a loop \mathcal{C}_n in $\mathcal{S}(3; 2)$ represented by the single-valued gauge choice in equation (14) that projects onto the loop C_n of complex two-planes in $G(3; 2)$. The connection one-form associated with this gauge reads

$$\mathcal{A} = \begin{pmatrix} 0 & 0 \\ 0 & \Omega(t)dt \end{pmatrix}, \quad (15)$$

which results in the holonomy matrix

$$U(C_n) = \mathbf{Z} = \begin{pmatrix} 1 & 0 \\ 0 & -1 \end{pmatrix} \quad (16)$$

for a single Rabi oscillation. Note that the matrix \mathbf{Z} is diagonal in the dark–bright basis but, in general, off-diagonal in the computational basis. An explicit calculation confirms that

$\sum_{k,l} \mathbf{Z}_{kl} |\zeta_k(0)\rangle \langle \zeta_l(0)| = \mathbf{n} \cdot \boldsymbol{\sigma}$. Similarly, for the composite path $C = C_{\mathbf{m}} \circ C_{\mathbf{n}}$, we obtain the $\sum_{k,l} \mathbf{U}_{kl}(C) |\zeta_k(0)\rangle \langle \zeta_l(0)| = \mathbf{n} \cdot \mathbf{m} - i\boldsymbol{\sigma} \cdot (\mathbf{n} \times \mathbf{m})$ from the holonomy matrix

$$U(C) = \mathbf{W}^\dagger \mathbf{Z} \mathbf{W} \mathbf{Z}. \quad (17)$$

Here, the unitary overlap matrix with components $\mathbf{W}_{kl} = \langle \zeta'_k(0) | \zeta_l(0) \rangle$ corresponds to an integration of a pure gauge connection one-form $i\mathbf{V}^\dagger d\mathbf{V}$ along any path \mathcal{D} in $\mathcal{S}(3; 2)$ that connects the initial bases $\{|\zeta_1(0)\rangle, |\zeta_2(0)\rangle\}$ and $\{|\zeta'_1(0)\rangle, |\zeta'_2(0)\rangle\}$ of $C_{\mathbf{n}}$ and $C_{\mathbf{m}}$, respectively [16]. In other words, the loop $C = C_{\mathbf{m}} \circ C_{\mathbf{n}}$ in $G(3; 2)$ is lifted to the loop $\mathcal{C} = \mathcal{D}^{-1} \circ C_{\mathbf{m}} \circ \mathcal{D} \circ C_{\mathbf{n}}$ in $\mathcal{S}(3; 2)$, where the four path segments correspond to the four non-commuting factors on the right-hand side of equation (17).

We end this section with some remarks on the geometrical aspects of the idea put forward by Zhu and Wang (ZW) [17] to realize non-commuting quantum gates by implementing phase shift gates in different bases. To see how this works, consider the one-qubit phase shift gates $|k\rangle \rightarrow e^{i(2k-1)\gamma} |k\rangle$, $k = 0, 1$, and $|\pm\rangle \rightarrow e^{\pm i\gamma'} |\pm\rangle$, $|\pm\rangle = \frac{1}{\sqrt{2}}(|0\rangle \pm |1\rangle)$, where γ and γ' are the corresponding cyclic phases. These gates are non-commuting and can be used to implement any one-qubit transformation by varying γ and γ' . The dynamical phase contribution to γ and γ' can be eliminated either by employing rotating driving fields with fine-tuned parameters [17–19] or by driving the qubit along geodesics on the Bloch sphere by using composite pulses [20–22]. These techniques result in non-commuting gates solely dependent on the non-adiabatic geometric phases of the cyclic states.

There are several differences between the geometric phase gates in the ZW setting and non-adiabatic HQC proposed in the present work. Firstly, the ZW scheme utilizes holonomies generated by loops in $G(N; 1)$, which is a fundamentally different space than the relevant Grassmannian $G(3; 2)$ associated with the holonomies in equation (17). Secondly, the loops that result in non-commuting gates in the ZW scheme are based at different points in $G(N; 1)$, while in non-adiabatic HQC all gates are based at a single point in $G(3; 2)$, namely $M(0)$. Finally, while the dynamical phases vanish for all input states in non-adiabatic HQC, all input states except the cyclic ones pick up a non-zero dynamical phase in the geometric phase version of the ZW scheme.

5. Conclusions

In conclusion, we have developed a non-adiabatic generalization of HQC with the primary purpose of finding ways to construct universal sets of robust high-speed geometric quantum gates. We have demonstrated an explicit realization of a universal set of holonomic one- and two-qubit gates in non-adiabatic evolution in three-level Λ configurations. The scheme requires coherent control of fewer levels and behaves more simply under decay of the excited state compared to the holonomic gates proposed for adiabatic evolution in tripod configurations [3–5]. Our gate opens up the possibility of realizing experimentally universal quantum computation on short-lived qubits by purely geometric means.

Acknowledgments

This work was supported by the National Research Foundation and the Ministry of Education (Singapore). DMT acknowledges support from NSF China (grant no. 11175105) and the National Basic Research Program of China (grant no. 2009CB929400).

References

- [1] Zanardi P and Rasetti M 1999 Holonomic quantum computation *Phys. Lett. A* **264** 94
- [2] Wilczek F and Zee A 1984 Appearance of gauge structure in simple dynamical systems *Phys. Rev. Lett.* **52** 2111
- [3] Duan L M, Cirac J I and Zoller P 2001 Geometric manipulation of trapped ions for quantum computation *Science* **292** 1695
- [4] Faoro L, Siewert J and Fazio R 2003 Non-Abelian holonomies, charge pumping and quantum computation with Josephson junctions *Phys. Rev. Lett.* **90** 028301
- [5] Solinas P, Zanardi P, Zanghì N and Rossi F 2003 Semiconductor-based geometrical quantum gates *Phys. Rev. B* **67** 121307
- [6] Wang X B and Keiji M 2001 Nonadiabatic conditional geometric phase shift with NMR *Phys. Rev. Lett.* **87** 097901
- [7] Aharonov Y and Anandan J 1987 Phase change during a cyclic quantum evolution *Phys. Rev. Lett.* **58** 1593
- [8] Anandan J 1988 Non-adiabatic non-Abelian geometric phase *Phys. Lett. A* **133** 171
- [9] Fleischhauer M and Manka A S 1996 Propagation of laser pulses and coherent population transfer in dissipative three-level systems: an adiabatic dressed-state picture *Phys. Rev. A* **54** 794
- [10] Sørensen A and Mølmer K 1999 Quantum computation with ions in thermal motion *Phys. Rev. Lett.* **82** 1971
- [11] Bremner M J, Dawson C M, Dodd J L, Gilchrist A, Harrow A W, Mortimer D, Nielsen M A and Osborne T J 2002 Practical scheme for quantum computation with any two-qubit entangling gate *Phys. Rev. Lett.* **89** 247902
- [12] Florio G, Facchi P, Fazio R, Giovannetti V and Pascazio S 2006 Robust gates for holonomic quantum computation *Phys. Rev. A* **73** 022327
- [13] Lupo C, Aniello P, Napolitano M and Florio G 2007 Robustness against parametric noise of nonideal holonomic gates *Phys. Rev. A* **76** 012309
- [14] Johansson M, Sjöqvist E, Andersson L M, Ericsson M, Hessmo B, Singh K and Tong D M 2012 Robustness of non-adiabatic holonomic gates arXiv:1204.5144v1
- [15] Bengtsson I and Życzkowski K 2006 *Geometry of Quantum States* (Cambridge: Cambridge University Press) chapter 4.9
- [16] Kult D, Åberg J and Sjöqvist E 2006 Noncyclic geometric changes of quantum states *Phys. Rev. A* **74** 022106
- [17] Zhu S-L and Wang Z D 2002 Implementation of universal quantum gates based on nonadiabatic geometric phases *Phys. Rev. Lett.* **89** 097902
- [18] Zhu S-L and Wang Z D 2003 Universal quantum gates based on a pair of orthogonal cyclic states: application to NMR systems *Phys. Rev. A* **67** 022319
- [19] Zhu S-L and Zanardi P 2005 Geometric quantum gates that are robust against stochastic control errors *Phys. Rev. A* **72** 020301
- [20] Solinas P, Zanardi P, Zanghì N and Rossi F 2003 Nonadiabatic geometrical quantum gates in semiconductor quantum dots *Phys. Rev. A* **67** 052309
- [21] Tian M, Barber Z W, Fischer J A and Babbitt W R 2004 Semiconductor-based geometrical quantum gates *Phys. Rev. A* **69** 050301
- [22] Ota Y and Kondo Y 2009 Composite pulses in NMR as nonadiabatic geometric quantum gates *Phys. Rev. A* **80** 024302